Biosensors and Bioelectronics 124–125 (2019) 25–32

Contents lists available at ScienceDirect

Biosensors and Bioelectronics

journal homepage: www.elsevier.com/locate/bios

A cell viability assessment approach based on electrical wound-healing impedance characteristics

Mingji Wei[a], Yecheng Zhang[a], Guoxiao Li[a], Ying Ni[b], Siqi Wang[c], Fei Zhang[a], Rongbiao Zhang[a,*], Ning Yang[a,*], Shihe Shao[b], Pan Wang[d]

[a] School of Electrical and Information Engineering, Jiangsu University, Zhenjiang, Jiangsu 212013, China
[b] School of Medicine, Jiangsu University, Zhenjiang, Jiangsu 212013, China
[c] School of Pharmacy, Jiangsu University, Zhenjiang, Jiangsu 212013, China
[d] Research Center of Fluid Machinery Engineering and Technology, Jiangsu University, Jiangsu 212013, China

ARTICLE INFO

Keywords:
Cell viability
Cell proliferation
Electrical wound-healing assay
Impedance characteristics
Biosensors

ABSTRACT

Cell viability evaluation is very meaningful for cancer treatment and cell proliferation is an effective evaluation criterion for cell viability. Traditionally, cell proliferation rate is obtained only by monitoring for several cell cycles (about 12 h) and yet there is no rapid assessment method to evaluate cell proliferation. In this paper, a rapid, real-time and online assessment approach (about 12.5 min) of cell proliferation based on electrical wound-healing impedance characteristics is proposed to evaluate the cell proliferation rate and improve cell viability assessment. The electrical wounding threshold u_{th} is firstly studied, then an electrical signal ($u_1 < u_{th}$) is applied to analyze cell recovery impedance characteristics, next an electrical signal ($u_2 > u_{th}$) is applied to wound cells on the electrodes to death. The real-time monitoring of cell proliferation is realized by Chi660E. The results indicate that the speed of cell recovery and proliferation become slower with a higher concentration of H_2O_2 added. On this basis, a model of the relationship between cell recovery impedance characteristics and cell proliferation is built for cell proliferation evaluation. Finally, the effect of temperature on cell recovery is also discussed to provide theoretical support for influencing factors of the biosensor design.

1. Introduction

Cancer is the leading cause of death all over the world. As was previously described in (Rodriguez and Pennington, 2018), there were 14.1 million new cancer cases and 8.2 million cancer deaths in 2012 worldwide. In order to improve the precision of reagent dosage for cancer treatment, cell viability requires to be precisely assessed (Zhang et al., 2018). Traditionally, cell viability means the percentage of live cells in total cells (Yang et al., 2016; Zhang et al., 2018), however, this evaluation method of cell status is unilateral and inaccurate for cancer treatment. Here, cell viability means a basic process for the increase in cell number by cell development and division (cell proliferation) (Xu et al., 2016). Although researches on cell viability are becoming a trend for precision medicine (Ren et al., 2015; Uhrin et al., 2018), in fact, the cell proliferation rate is only obtained by monitoring for several cell cycles, and yet there is no rapid, real-time and online assessment method to evaluate cell proliferation.

Among many evaluation methods of cell viability, the impedance sensing method using electric cell-substrate impedance sensing (ECIS) is widely accepted as a label-free, non-invasive, real-time and quantitative analytical method to assess cell status (Xu et al., 2016; Zhang et al., 2018). Impedance-related measurements use electric impedance spectroscopy (EIS) ranging from 1 Hz to 10^6 Hz for many different forms of analysis. Also, some papers use a frequency of 4 kHz to realize real-time monitoring of cell proliferation and migration (CR et al., 2004; Stolwijk et al., 2011; Yang et al., 2016). The approach returns highly quantitative data regarding cell dynamic events like cell adhesion, proliferation and migration in relatively short times and with a minimum of labor and cell culture manipulations (CR et al., 2004; Koo and Yun, 2016). A weak (< 1 μA) AC signal is applied to the interdigitated electrode structures (IDES) of ECIS when measurement frequency ranges from 1 to 40 kHz (CR et al., 2004). As was described in (I and CR, 1991) before, when the cells attach and spread on the electrode surface, they alter the effective area available for current flow causing as much as an 8-fold increase in the impedance of the system. However, this small current results in a voltage drop of only a few millivolts across the small electrode and the measurement are noninvasive for cells (CR et al., 2004). So, this method is very useful for analysis and

* Corresponding authors.
E-mail addresses: zrb@ujs.edu.cn (R. Zhang), yangn@ujs.edu.cn (N. Yang).

https://doi.org/10.1016/j.bios.2018.09.080
Received 13 June 2018; Received in revised form 20 September 2018; Accepted 21 September 2018
Available online 22 September 2018
0956-5663/

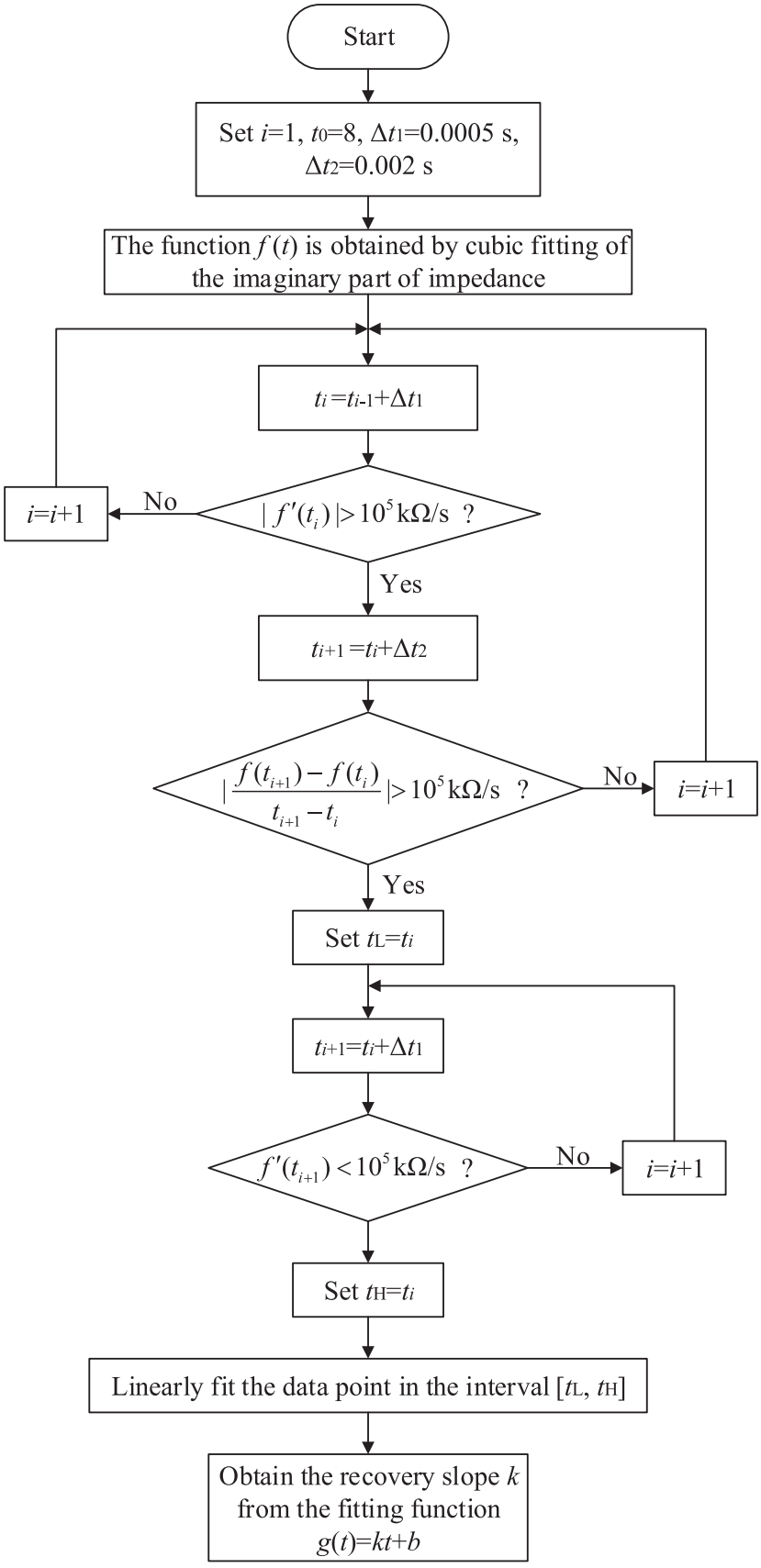

Fig. 1. Flow chart of the calculation of cell recovery slope *k*.

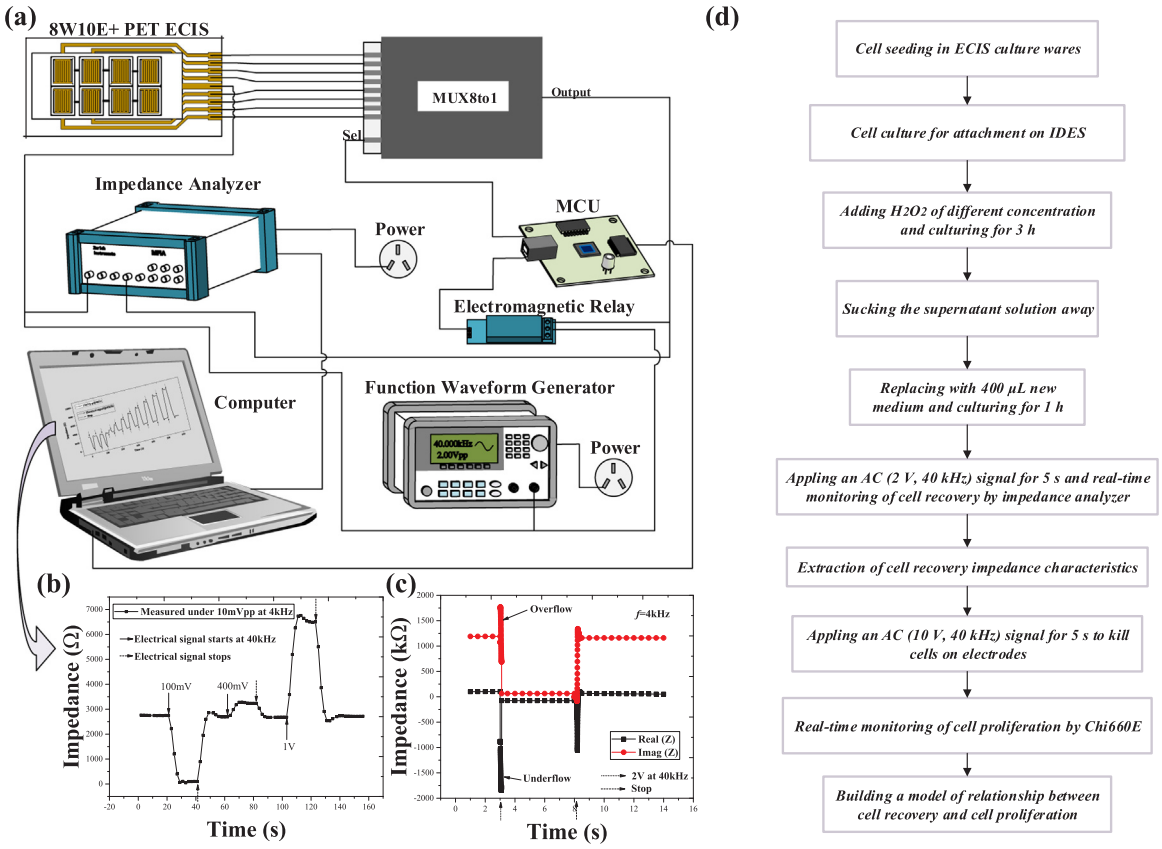

Fig. 2. Diagram of the experimental platform. (a) The multiplexer MUX8to1 connected to ECIS is chosen as a gating switch to select one from eight signals. Impedance analyzer or Chi660E is connected with the common port of ECIS on one side and output port of MUX8to1 on another side. Function Waveform Generator is connected in parallel with impedance analyzer to apply an AC signal to ECIS culture wares. Electromagnetic Relay is connected with MCU to control the application time of Function Waveform Generator. (b) Experiment data measured by Chi660E are recorded by a computer for subsequent processing. (c) Experiment data measured by impedance analyzer are recorded. (d) Schematic diagram of the whole assay process.

real-time monitoring of adherent cells (Xu et al., 2016).

Electrical wound-healing assay using impedance sensing method was carried out in many papers (Castellví et al., 2017; CR et al., 2004; García-Sánchez et al., 2018; Ghosh et al., 1993; Koo and Yun, 2016; M, 2009; Stolwijk et al., 2011; Veiga et al., 2005; Wegener et al., 2002; Yang et al., 2016). Among them, (Castellví et al., 2017; Ghosh et al., 1993; Stolwijk et al., 2011; Wegener et al., 2002) studied the electropermeabilization of adherent cells by constantly monitoring the impedance of adherent cells to detect the small changes in cell morphology, cell motion, and membrane resistance. (CR et al., 2004; García-Sánchez et al., 2018; Koo and Yun, 2016; M, 2009; Veiga et al., 2005; Yang et al., 2016) studied the electrical wound-healing process by measuring impedance in real time after wounding was created by high current. The authors above have done many meaningful types of research and provided the basis for the study in this paper. We did some further researches to make the electrical wound-healing assay theoretical enough for the design of biosensors. In this paper, we have tried to build a model of a relationship between cell recovery impedance characteristics and cell proliferation rate under the same cell number but different cell viability. This approach can realize real-time and online monitoring by returning highly quantitative data about cell electrical wound-healing impedance characteristics in relatively short times and with a minimum of labor and cell culture manipulations. Meanwhile, this procedure is highly reproducible and quantitative and it can provide theoretical support for the design and fabrication of biosensors.

2. Materials and methods

2.1. Cell culture

Human gastric cancer cells (SGC-7901) are provided by Medical School, Jiangsu University (China) and they are cultured in Dulbecco's Modified Eagle's Medium (DMEM) supplemented with 10% fetal bovine serum (FBS) (Gibco, USA) at 37 °C and 5% CO_2 inside a Water Jacketed CO_2 Incubator (Heal Force®). Cell culture medium (DMEM with 10% FBS) is changed every 48 h. Cells are detached from cell culture dish using try-EDTA (Life Technologies GmbH, Darmstadt, Germany) for 2 min, and the cell culture medium is centrifuged at a speed of 600 rpm for 5 min. The supernatant solution is sucked away and changed for 3 mL new medium, and the new medium containing cells is mixed uniformly. 400 μL new medium is dripped into each culture ware of 8W10E + PET ECIS, where polyethylene terephthalate (PET) is a type of film. Gastric cancer cells are completely attached to the IDES of ECIS after cultured in Water Jacketed CO_2 Incubator for 12 h.

2.2. Cell electrical wounding assay

400 μL new medium containing cells is dripped into each culture ware of 8W10E+ PET ECIS. After cultured for 24 h, gastric cancer cells are attached to IDES of ECIS and they grow to fill the exposed electrodes. We have prepared four concentrations of H_2O_2 (0, 50, 100, 150 μmol/L), 30 μL of each solution is dripped into ECIS culture ware cultured for 3 h. The supernatant solution is sucked away and 400 μL new medium (DMEM with 10% FBS) is dripped into ECIS and cultured for 1 h.

The threshold measurement assay is carried out to study the ability of cells withstanding voltage. Firstly, an initial electrical signal (2 V, 40 kHz) is applied to culture wares of ECIS for 5 s, when the damage to cell layer seems complete (CR et al., 2004). Then, the electrical signal increases at an interval of 100 mV until the impedance measured by Chi660E at 4 kHz suddenly drops and is not recovering soon. The spacing interval between two electrical signals is 20 s for cell complete recovery.

The model is built according to the following steps: (1) Set up the control group. An AC signal of 2 V at 40 kHz is applied to four culture wares of ECIS (without H_2O_2), which are considered as the control groups. Meanwhile, the real-time monitoring of impedance is realized by impedance analyzer; (2) Establish cell viability gradient. After different levels of H_2O_2 are dripped into culture wares incubated for 3 h, the supernatant solution is sucked away and replaced with 400 μL new medium (DMEM with 10% FBS). Then ECIS is cultured in Water Jacketed CO_2 Incubator for 1 h. (3) Wound cells and record the recovery impedance. An AC signal of 2 V at 40 kHz is applied to four culture wares for 5 s and cell recovery impedances are recorded by an impedance analyzer. The rest time between two times of electrical wounding is 60 s. This procedure is repeated for five times to calculate an average result and the error bar. (4) Kill cells and monitor the cell proliferation. An AC signal (5 s) of 10 V at 40 kHz is applied to culture wares to kill cells on exposed electrodes. The real-time monitoring of cell proliferation is realized by Chi660E. The sample impedance divided by the impedance of control group is normalized (please see Fig. 2(d)).

2.3. Introduction of cell viability assessment method

The impedance of cell recovery from electrical wounding is recorded by an impedance analyzer. The imaginary part Z′ of impedance is fitted to calculate the slope k_i (i = 1, 2, …, n) of recovery curves. Where, the slope k_i is obtained by linear fitting in the interval $[t_{i1}, t_{i2}]$, where curve shows an approximately linear change. The detail steps are shown in Fig. 1. The fitting result shows in Fig. 4(b) and the formula is shown as follows:

$$y = kt + b \tag{1}$$

c_i is the corresponding concentration of H_2O_2 and the cell proliferation rate affected by the different concentration of H_2O_2 is defined as v_i, which means the velocity of cells proliferating to a normal level. The slope k_i is set as the x-axis and the velocity of cell proliferation v_i is set as the y-axis, as shown in Eq. (2).

$$\begin{cases} x = k_i \\ y = v_i \end{cases} \tag{2}$$

Then the scattered point (k_i, v_i) is quadratically fitted by OriginPro2016 shown as follows:

$$f(k_i) = v_i \tag{3}$$

The whole procedures include the electrical wounding time (~ 5 s), the cell recovery time (~ 15 ms) from electrical wounding, the rest time for complete recovery (~ 60 s) and the experimental data processing time (~ 10 s). Besides, the whole procedures are repeated ten times to obtain an average result (~ 12.5 min). Finally, we can calculate the cell proliferation rate using the average result based on the model (Eq. (3)).

2.4. Experimental set-up

In this paper, impedance analyzer, whose measurement period is 25 μs, was purchased from Zurich Instruments (Switzerland). Impedance analyzer is used for real-time monitoring of the cell recovery from electrical wounding. Chi660E electrochemical workstation, whose measurement period is 2 s at 4 kHz, was purchased from Chenhua Instrument (Shanghai China). Chi660E is used to monitor cell recovery, migration, and proliferation. 8W10E + PET ECIS was purchased from Applied BioPhysics (America).

The stimulus AC signal of V_{pp} (peak-to-peak) at 40 kHz is generated by SDG830 Function Waveform Generator (SIGLENT Technologies, China). The multiplexer MUX8to1 is chosen as a gating switch to select one from eight signals. The electromagnetic Relay is chosen as a single path switch to control the on-off between the microcontroller unit (MCU) and Function Waveform Generator (see Fig. 2(a)). Data measured by Chi660E (see Fig. 2(b)) and impedance analyzer (see Fig. 2(c)) are recorded by a computer for subsequent processing. Besides, an AC signal of 2 V at 40 kHz starts to be applied from a time coordinate of 3 s, and it lasts for 5 s as shown in Fig. 2(c). However, it is the cell recovery interval that is important for the results instead of the so-called time coordinate. For convenience, we stop electrical wounding at a time coordinate of 8 s and we can see the cell recovery around 8.119 s–8.127 s (see Fig. 4). The whole assay process can be seen in Fig. 2(d).

3. Results and discussion

3.1. The threshold of adherent cells withstanding voltage

In this paper, we need to find the impedance characteristics of cell recovery and cell proliferation. So, the threshold u_{th} of adherent cells withstanding voltage is needed to determine the electrical signal u_1 ($< u_{th}$) to study characteristics of cell recovery and determine the electrical signal u_2 ($> u_{th}$) wounding cells to death to study cell proliferation and migration.

8W10E + PET ECIS is used for real-time monitoring of the cell electrical wound-healing process, as is shown in Fig. 3(a). A thin film of PET is attached to the IDES of ECIS. The PET has five round holes (d = 250 μm) over electrodes, allowing the electrodes to be exposed to outside environment. The whole process of cell wound-healing assay is shown in Fig. 3(a): (1) Cells are attached to PET film and electrodes after cultured for 24 h; (2) Cells are wounded using u_1 ($< u_{th}$) at 40 kHz for 5 s and the real-time monitoring of the wound-healing process is realized by impedance analyzer; (3) Then cells are stimulated to death using u_2 ($> u_{th}$) at 40 kHz for 5 s; (4) Cell proliferation and migration are monitored by Chi660E at a measurement interval of 0.5 h. The schematic diagram of the whole process can be seen in Fig. 2(d).

Fig. 3(b) shows adherent cells on IDES on the scale bar of 500 μm and 125 μm. We can know from (Asphahani et al., 2008; Zhang et al., 2017) that, the intercellular space will affect the equivalent circuit model of adherent cells, which in turn leads to the changes of the effective voltage between cells causing an effect on the cell recovery. Thus, when cells are cultured for 24 h to overspread the surface of electrodes, we can consider the cells number and the intercellular spaces as the same. In this paper, we have tried to find a relationship between cell recovery impedance characteristics and cell proliferation rate under the same cell number but different cell viability.

Before the threshold assay was carried on, we have first studied the optimal measurement frequency, as is shown in Fig. 3(c). (García-Sánchez et al., 2018) reports the comparative analysis of three different cell lines subjected to electroporation pulses using EIS from 5 kHz to 1.3 MHz. As was described in (Wegener et al., 2000, 2002), authors studied different situations at electrode surface by calculating the evolution of resistance and capacitance value as a function of surface coverage for the three major measuring frequencies of 400 Hz, 4 kHz, and 40 kHz. In this paper, we have verified the optimal result of 4 kHz, as was also described in some papers (CR et al., 2004; Ghosh et al., 1993; Stolwijk et al., 2011; Yang et al., 2016). We can see from Fig. 3(c) that impedance measured at 4 kHz is more stable than that measured at 1 kHz and 400 kHz. Meanwhile, resonance (marked with a broken circle in Fig. 3(c)) will happen when the impedance is measured at 40 kHz (electrical wounding frequency is 40 kHz).

In order to study the ability of cells withstanding voltage, an initial

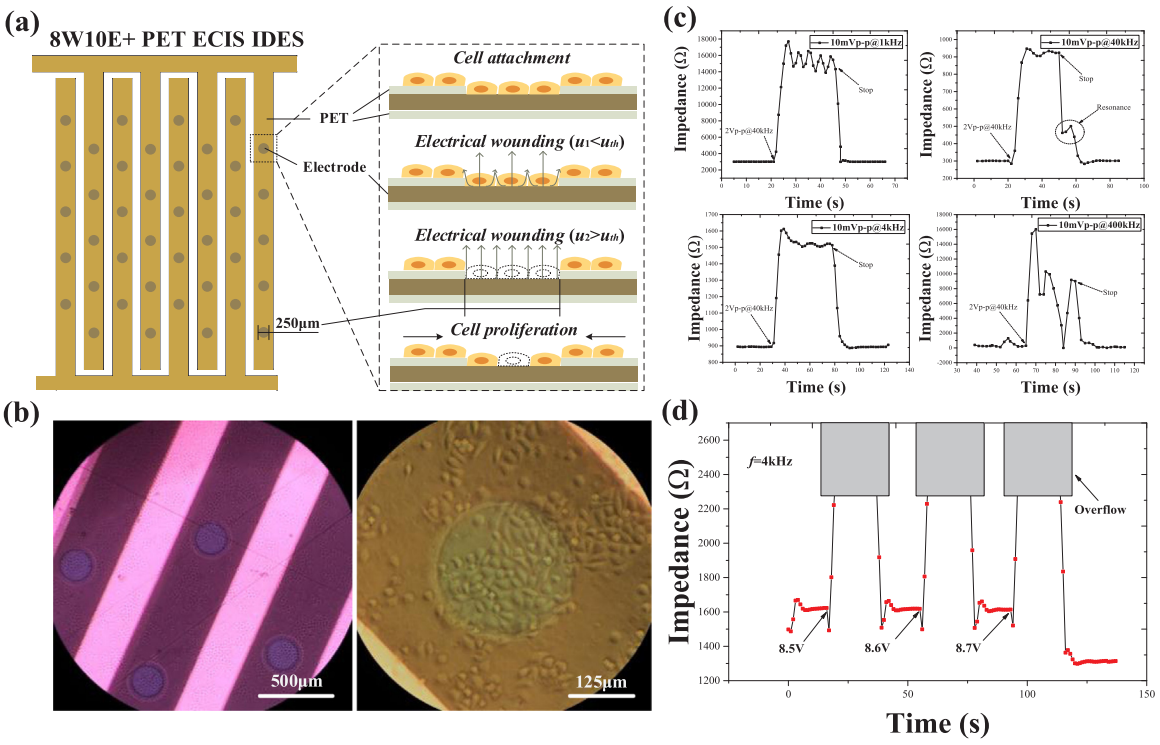

Fig. 3. The process of the electrical wounding assay. (a) A layer of PET is attached to the surface of 8W10E + PET ECIS IDES, and the PET has five round holes above each electrode, allowing the electrode to be exposed to the outside environment. Cells attached on the electrodes after cells are seeded in ECIS culture wares for 24 h. Then cells recover quickly after they are wounded using 2 V ($< u_{th}$) at 40 kHz. Cells are electrically wounded to death when the electrical signal reaches to 10 V ($> u_{th}$) at 40 kHz. Then cells on PET migrate to the area of electrical wounding. (b) Photos of cells attached to IDES. The scale bars represent 500 μm and 125 μm respectively. (c) The optimal measurement frequency is tested, and 4 kHz seems more stable and suitable. (d) Threshold u_{th} of adherent cells withstanding voltage is tested by Chi660E and the u_{th} is 8.7 V.

electrical signal of 2 V at 40 kHz is applied to culture wares of ECIS for 5 s. The duration of the electrical signal was previously discussed in (CR et al., 2004) that the damage to cell layer seems complete. Then, the electrical signal increases at an interval of 100 mV until the impedance measured by Chi660E at 4 kHz suddenly drops and does not recover soon. As was described in (Batista and Miklavčič, 2017), when biologic cells are exposed to a pulsed electric field of sufficient amplitude, their plasma membrane permeability increases. So, the spacing interval between two electrical signals is 20 s for cell complete recovery. If the transmembrane potential is raised further, irreversible membrane damage takes place culminating in cell death (Ghosh et al., 1993). We can see from Fig. 3(d) that the threshold u_{th} is 8.7 V. Overflow (marked in the grey area) will happen when the applied electrical signal increases to 3 V or more. In addition, cells seem to adapt to electrical stimulation. Under continuous application of an electrical signal, the threshold u_{th} may larger than 8.7 V (data not shown). Again, cells of different proliferation rate have different abilities to withstand voltage. However, those thresholds are far larger than 5 V, as was previously described in (CR et al., 2004; Stolwijk et al., 2011). In addition, the threshold is highly dependent on the type of cells.

3.2. The relationship between cell electrical wound-healing characteristics and cell proliferation

As was previously described in (Zhang et al., 2018), cell viability means the percentage of live cells in total cells. However, the cancer cell tolerance to the drug is usually somewhat different under the same cell number, so we defined cell proliferation as cell viability here and studied a rapid, real-time, online and automatic method to evaluate cell proliferation. In this paper, we have tried to study a relationship between cell electrical wound-healing characteristics and cell proliferation for cell viability assessment. As we all know, cancer cells are more sensitive to H_2O_2 than normal cells and appropriate concentration of H_2O_2 (0, 50, 100, 150 μmol/L) can affect cancer cell proliferation (Roy et al., 2016). Firstly, an AC signal (2 V, 40 kHz) is applied to sample groups in ECIS culture wares for 5 s. The real-time monitoring of cell recovery is realized by an impedance analyzer after the AC signal is stopped. Data in some literature (Ghosh et al., 1993) showed that the time taken for complete recovery varies widely from a few seconds to a few hours due to different types of cells, and SGC-7901 cancer cells in this paper are found need 40–60 s complete recovery time. Then cells on the electrodes are electrical wounded to death using a signal of 10 V at 40 kHz. Before these microscopic observations, we have speculated that the wounded cells would round and lift from the electrode, but this occurrence has not been observed for cells in this assay. In fact, (CR et al., 2004) have already verified that the cells are killed and replaced rather than being transiently damaged. On wounding, there is a subtle change in the appearance of the cells as they show reduced contrast, with less clearly defined cell boundaries. As was previously described in (CR et al., 2004), cells on PET (see Fig. 3(a)) proliferate and migrate beneath the lifted cell layer or displace the wounded cells in a snow-plow-like fashion. Chi660E is used for real-time monitoring of this dynamic event above.

Impedance characteristics of cell recovery measured by impedance analyzer are analyzed in Fig. 4. The real part of impedance Z′ responds to electrical stimulation during cell recovery as shown in Fig. 4(a). The changing rate of Z′ is related to the concentration of H_2O_2. Low concentration of H_2O_2 (< 500 μmol/L) might weaken adhesion of cell membrane, the activity of cell proliferation rather than wounding them to death. We can see from Fig. 4(b), the impedance of cell recovery shows a significant effect from 0 μmol/L H_2O_2. In fact, compared with the control group (400 μL medium), the sample group (430 μL medium) additionally contains 30 μL of 0 μmol/L H_2O_2. This may lead to a change of solution conductivity and then the effective voltage changes

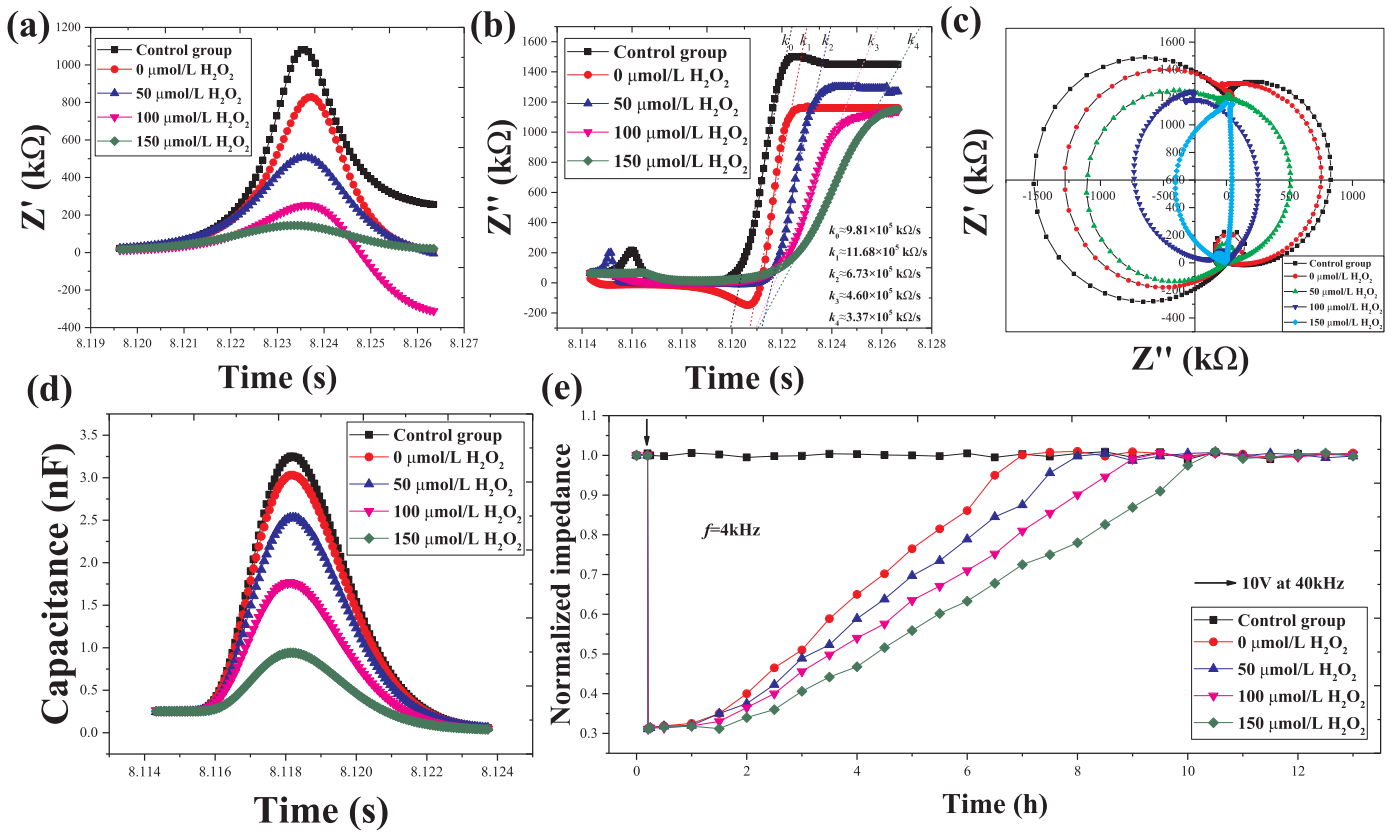

Fig. 4. The relationship between cell electrical wound-healing characteristics and cell proliferation. An electrical signal of 2 V at 40 kHz is applied to ECIS. Original 400 μL of cell medium is considered as a control group. Four ECIS culture wares contain 30 μL of 0 μmol/L, 50 μmol/L, 100 μmol/L, and 150 μmol/L H_2O_2 respectively. (a) The real part of the impedance response to electrical stimulation during cell recovery. (b) The imaginary part of the impedance response to electrical stimulation during cell recovery. (c) Nyquist diagram response to electrical stimulation during cell recovery. (d) Equivalent capacitance response to electrical stimulation during cell recovery. (e) The relationship between cell proliferation and concentration of H_2O_2 after cells on the electrodes are wounded to death by an electrical signal (10 V, 40 kHz).

as well. The slope of imaginary part Z″ diminishes with the increasing concentration of H_2O_2. The calculation of the slope k is shown in Fig. 1 in detail. We build a model of a relationship between cell recovery rate and cell proliferation as shown in Fig. 4(e). The Nyquist diagram is also drawn to analyze the model (see Fig. 4(c)). Obviously, the higher the H_2O_2 concentration level is, the larger the range of reaction the real part and imaginary part of impedance have. We can see from Fig. 4(a), (b) and (c), the process of cell recovery from electrical wounding finishes in a quite short time (within 15 ms), which is consistent with the description in (Castellví et al., 2017; Voyer et al., 2017). However, the whole detection time contains the electrical wounding time (~ 5 s), the cell recovery time (~ 15 ms) from electrical wounding, the rest time for complete recovery (~ 60 s) and the experimental data processing time (~ 10 s). And the whole procedures are repeated ten times to obtain an average result. In summary, the period of this method is about 12.5 min.

When the impedance of cell recovery is recorded by an impedance analyzer, we choose a resistance in parallel with a capacitance as an equivalent circuit. We can see from Fig. 4(d) that, the capacitance of the control group increases from ≈ 0.25 nF to 3.25 nF, the result is similar to what was described in (CR et al., 2004) before. Moreover, the equivalent capacitances of sample group show the same regular pattern as a Nyquist diagram. The capacitance of the sample group (150 μmol/L H_2O_2) increases merely from 0.25 nF to 0.95 nF as shown in Fig. 4(d). Fig. 4(e) shows that the normalized impedances of sample groups return to normal level after SGC-7901 cells are electrically wounded by 10 V at 40 kHz for 5 s. As was previously described in (CR et al., 2004), the time required for cell healing depends on the size of ECIS electrodes, so the speed of cell recovery should be identical if cell status is almost the same. A gradient of cell proliferation is built by different concentration of H_2O_2 and we have verified that the cell electrical wound-healing impedance characteristics are related to cell proliferation rate. By the way, these wound-healing curves are highly dependent on the type of cell being cultured (CR et al., 2004).

The scattered points (k, v) of the sample groups are quadratically fitted by OriginPro2016, as shown in Fig. 5. Where, k_i is the imaginary part slope of cell recovery impedance (see Fig. 4(b)), which is calculated according to Fig. 1. In fact, the sample groups include four groups

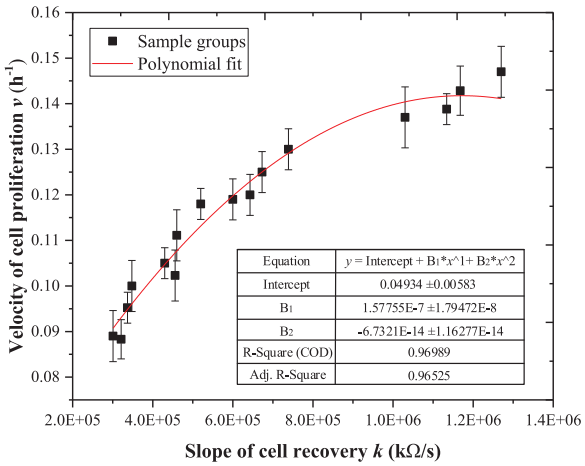

Fig. 5. Quadratic fitting of sample groups with different concentrations of H_2O_2 ($P < 0.05$, $N = 20$).

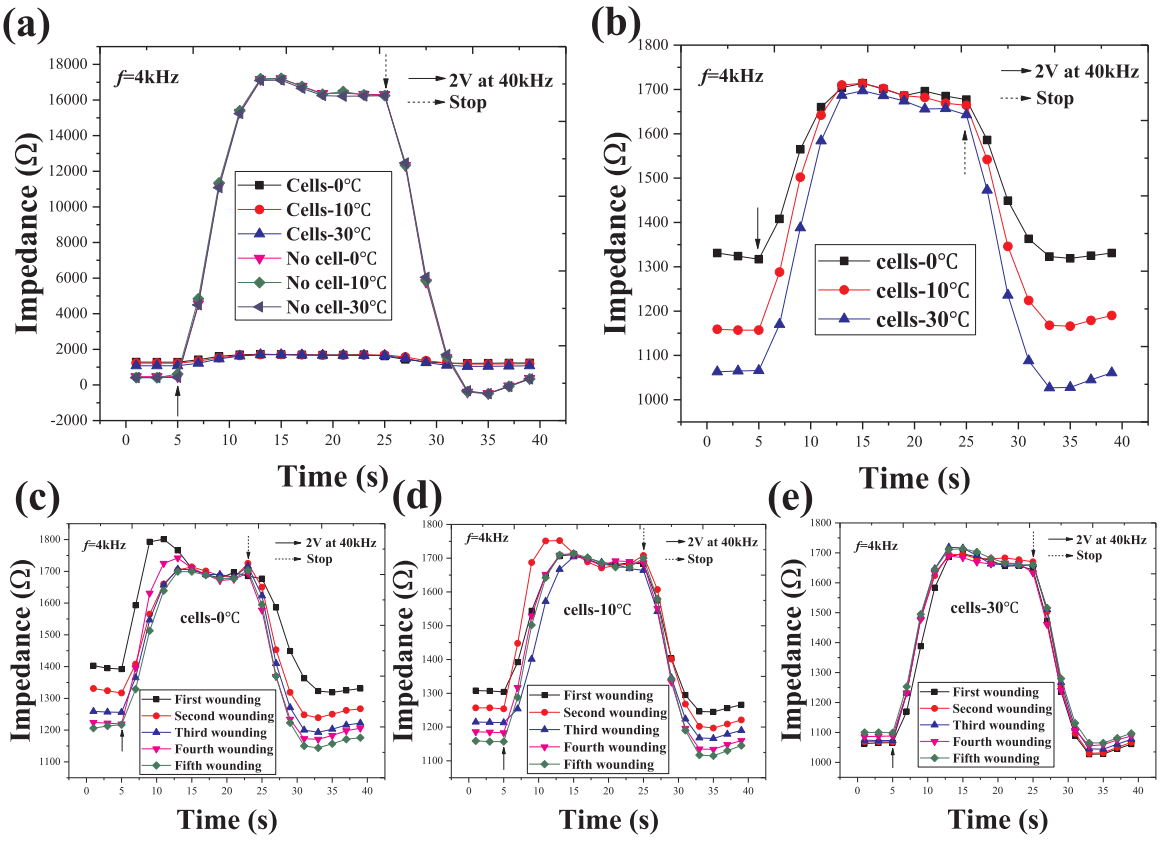

Fig. 6. Effect of temperature to adherent cells. An electrical signal (2 V, 40 kHz) is applied to ECIS culture wares, and the real-time monitoring of impedance is realized by Chi660E at 4 kHz. (a) Recovery impedances of cell attachment and no cell attachment are measured at different temperatures. (b) Recovery impedances of adherent cells are measured at 0, 10, 30 °C. (c) A sample group is wounded five times at 0 °C. The interval between damages is 20 s (d) A sample group is wounded five times at 10 °C. (e) A sample group is wounded five times at 30 °C.

and each sample group includes five repeated samples, which are used to calculate an average result and the error bar. Five digits of fitting precision automatically produced by software can be seen from Fig. 5. However, we can know from (Bolten, 2015; Cole, 2015) that too many digits of fitting precision actually does hurt the accuracy of experimental results, because the actual result of cell proliferation velocity cannot be predicted to five digits of precision from the slope of cell recovery. Thus, the two-digit precision of Intercept and B_1 and one-digit precision of B_2 are kept to improve the ability to convey information as shown in Eq. (4). Where, Intercept = 0.05 ± 0.02, B_1 = 1.58 ± 0.28E-7, B_2 = −6.7 ± 2.7E-14.

$$y = 0.05 + 1.58 \times 10^{-7}x - 6.7 \times 10^{-14}x^2 \quad (4)$$

Obviously, we can know from the Fig. 5 and Eq. (4) that the relationship between the velocity of cell proliferation and speed of cell recovery is not linear. The coefficient B_1 represents the linear relationship, however, the change rate of cell proliferation velocity slows down gradually with the increase of cell recovery speed. Thus, the coefficient of quadratic term B_2 is introduced to correct the data deviation from reality.

Commonly, healthy cell status shows a strong cell proliferation and an easy recovery from electrical or mechanical wounding. However, cell proliferation rate requires long-time tracking of several cell cycles, while the cell electrical wound-healing assay is completed within a quarter of an hour. The quadratic fitting function (see Eq. (4)) can be used to predict the velocity of cell proliferation from cell electrical wound-healing assay. Readers can conclude some regular patterns between two inherently related physical phenomena according to the method proposed in this paper, such as the relationship between cell adhesion and cell viability.

The R-Square (COD) is the coefficient of multiple determination and the Adj. R-Square is the degree of freedom adjusted R-Square. Both of them indicate a better fit when they are close to 1. We can see from Fig. 5 that the COD is ~ 0.97 and the Adj. R-Square is ~ 0.97, it means a quite perfect fitting to scattered point (k, v). Meanwhile, the probability P, that the differences between samples causing by sampling errors, is less than 0.05 (N = 20). It means the results are statistically significant.

As we all know, it is unilateral to use the percentage of live cells in total cells to assess cell viability, and cell proliferation is a more effective evaluation criterion of cell status. The relationship between the slope of cell recovery imaginary part Z′ and the cell proliferation rate is quadratically fitted as shown in Eq. (4), based on which a biosensor for cell proliferation assessment can be designed and fabricated.

3.3. Effect of temperature on electrical wound-healing cells

As is widely known, cell status including cell viability, cell adhesion, and cell proliferation is strongest at ≈ 37 °C. We have tried to study the effect of temperature on electrical wound-healing cells and provide theoretical support for influencing factors of biosensors design.

We used the same sample group to study cell wound-healing characteristics (2 V, 40 kHz) at 0, 10, 30 °C respectively. The recovery rate of wounded cells increases with temperature increment (< 37 °C), it means cell status is strongest at 37 °C (data not shown). ECIS culture ware with no cell is considered as the control group and the impedance measured by Chi660E has little changes (see Fig. 6(a)). As is shown in Fig. 6(b), the impedance of adherent cells decreases with the temperature increment. In fact, as the cells attach and spread on the IDES of ECIS, their membranes constrict the current forcing it to flow beneath and between the cells, resulting in large increases in impedance (CR

et al., 2004). Higher temperature (< 37 °C) enhances the constriction of cell membranes, which leads to the increase of impedance.

We can see from Fig. 6(c) and (d), the impedance cannot return to normal level within 20 s at a lower temperature, and the impedance will decrease every time when cells are electrically wounded by 2 V at 40 kHz. However, cells can quickly recover from electrical stimulation when the temperature is higher than 30 °C (< 37.5 °C). By the way, the imaginary part of impedance seems little changes at different temperatures (data not shown). Finally, we find that the Chi660E is suitable for long-term monitoring and the Zurich Impedance Analyzer is suitable for instantaneous changes.

4. Conclusions

In this paper, a rapid, real-time and online assessment approach of cell proliferation based on electrical wound-healing impedance characteristics is proposed to evaluate the cell proliferation rate and improve cell viability assessment. The results indicate that the velocity of cell proliferation shows a regular pattern with the speed of cell recovery from electrical wound-healing. On this basis, a cell viability evaluation model is built to predict the cell proliferation rate from cell electrical wound-healing assay. Besides, the effect of temperature on cell recovery is also discussed in this paper.

Significantly, the time taken for complete recovery varies widely from a few seconds to a few hours due to different types of cells, thus the electrical wounding and rest time of various cells is urged to study in the future. Furthermore, impedance drift may occur when the impedance analyzer is overloaded, so it is necessary to study appropriate electrical wounding signals to evaluate cell status more quantitatively and repeatedly.

Acknowledgements

This work was financially supported by the National Natural Science Foundation of China [grant No. 61673195] and the Priority Academic Program Development of Jiangsu Higher Education Institutions (PAPD).

References

Asphahani, F., Thein, M., Veiseh, O., Edmondson, D., Kosai, R., Veiseh, M., Xu, J., Zhang, M., 2008. Biosens. Bioelectron. 23 (8), 1307–1313.
Batista, T.N., Miklavčič, D., 2017. Bioelectrochemistry 166–182.
Bolten, R., 2015. J. Corp. Account. Financ. 26 (5), 45–56.
Castellví, Q., Mercadal, B., Ivorra, A., 2017. In: Miklavčič, D. (Ed.), Handbook of Electroporation. Springer International Publishing, Cham, pp. 671–690.
Cole, T.J., 2015. Arch. Dis. Child. 100 (7), 608–609.
CR, K., J, W., SR, W., I, G., 2004. Proc. Natl. Acad. Sci. USA 101 (6), 1554–1559.
García-Sánchez, T., Bragós, R., Mir, L.M., 2018. Biosens. Bioelectron. 117, 207.
Ghosh, P.M., Keese, C.R., Giaever, I., 1993. Biophys. J. 64 (5), 1602–1609.
I, G., CR, K., 1991. Proc. Natl. Acad. Sci.USA 88 (17), 7896–7900.
Koo, Y., Yun, Y., 2016. Mater. Sci. Eng. C Mater. Biol. Appl. 69, 554–560.
M, Z, 2009. Semin. Cell Dev. Biol. 20 (6), 674–682.
Ren, X., Tapias, L.F., Jank, B.J., Mathisen, D.J., Lanuti, M., Ott, H.C., 2015. Biomaterials 52 (1), 103–112.
Rodriguez, H., Pennington, S.R., 2018. Cell 173 (3), 535–539.
Roy, M., Jin, G., Pan, J.H., Seo, D., Hwang, Y., Oh, S., Lee, M., Kim, Y.J., Seo, S., 2016. Sens. Actuators B Chem. 224, 577–583.
Stolwijk, J.A., Hartmann, C., Balani, P., Albermann, S., Keese, C.R., Giaever, I., Wegener, J., 2011. Biosens. Bioelectron. 26 (12), 4720–4727.
Uhrin, P., Wang, D., Mocan, A., Waltenberger, B., Breuss, J.M., Tewari, D., Mihaly-Bison, J., Huminiecki, Ł., Starzyński, R.R., Tzvetkov, N.T., 2018. Biotechnol. Adv.
Veiga, V.F., Nimrichter, L., Teixeira, C.A., Morales, M.M., Alviano, C.S., Rodrigues, M.L., Holandino, C., 2005. Cell Biochem. Biophys. 42 (1), 61–74.
Voyer, D., Silve, A., Mir, L.M., Scorretti, R., Poignard, C., 2017. Bioelectrochemistry 119, 98.
Wegener, J., Keese, C.R., Giaever, I., 2000. Exp. Cell Res. 259 (1), 158–166.
Wegener, J., Keese, C.R., Giaever, I., 2002. Biotechniques 33 (2) (357-350).
Xu, Y., Xie, X., Duan, Y., Wang, L., Cheng, Z., Cheng, J., 2016. Biosens. Bioelectron. 77 (77), 824–836.
Yang, J.M., Chen, S.W., Yang, J.H., Hsu, C.C., Wang, J.S., 2016. Comput. Biol. Med. 69, 134–143.
Zhang, R., Wei, M., Chen, S., Li, G., Zhang, F., Yang, N., Huang, L., 2018. Biosens. Bioelectron. 110, 193–200.
Zhang, X., Wang, W., Nordin, A.N., Li, F., Rivera, A., Jang, S., Voiculescu, I., 2017. Sens. Actuators B Chem.